A Shading Model of Parallel Cylindrical Light Sources

Tomoyuki Nishita, Shinichi Takita, and Eihachiro Nakamae

ABSTRACT

In many industrial designs, such as automobiles and electrical products, evaluating the quality of curved surfaces in the design is very important. If the designer can confirm shapes of curved surfaces visually, working with photo-realistic computer generated images, the designer's "sense" is well utilized. In this paper we will demonstrate method for producing images which can be used by designers to evaluate the visual quality of free-form curved surfaces. The method uses the reflected images of cylindrical light sources. It is important that curved surfaces be displayed accurately, without polygonal approximation, and that the generated images be photo-realistic images, including shadows. The shading model presented in this paper satisfies these requirements.

Many offices, classrooms, and factories are lit with multiple fluorescent lamps arrayed in parallel rows on the ceiling. The shading technique presented in this paper is applicable to estimation of illuminance distribution in such an environment. Our method performs hidden surface removal and shadowing of curved surfaces without polygonal approximation, yielding accurate display.

Keywords: Cylindrical light sources, quality of curved surfaces, shadows, penumbra, Bézier surfaces.

1 INTRODUCTION

An accurate and photo-realistic shading method for curved surfaces which appeals directly to the designer's visual sense is discussed in this paper. In particular, smoothness and continuity between curved patches are especially important in shape designs, and many mathematical methods addressing these problems have been developed. For a designer attempting to evaluate a shape, however, intuitive and visual methods may be desired. In current automobile design, designers evaluate the quality of auto bodies by observing reflected images of parallel fluorescent lamps. This procedure requires a real physical model to be produced, and making modifications or adjustments to the shape is a time-consuming and expensive process. Furthermore, large scale equipment is used to adjust the positions of the light sources and/or the auto body to examine reflections in various positions. It is clear that if evaluation could be carried out using a computer graphic simulation, time and expenses could be saved and the quality of the design improved by increasing the speed of the modify/evaluate/modify cycle. Before this can be accomplished, however, the following problems must be solved.

(1) An accurate representation of the curved surface must be displayed without approximation, faithful to the designed shape.

(2) Display of accurate reflected images to display precise features of the curved surfaces must be realized at a practical computational cost.

(3) The displayed image must include shadows and have a highly realistic appearance adequate to fool the designer's senses into a feeling of being present in front of a real model.

Because conventional polygonal approximation can not produce accurate curved surfaces, a designer attempting to evaluate a design using such an approximation may be working with a surface considerably different than the actual design. Further, the smoothness of curved surfaces illuminated only by point or parallel light sources can not be evaluated precisely. Contour lines or highlight curves can be displayed as line drawings, but such drawings are not adequate to allow the designer's visual intuition to grasp the quality of the shape. Reflection lines (or highlight curves) can be used to detect irregularity of curved surfaces which are not brought out by contour lines. Reflection lines are essentially the reflected image of infinitely long, linear light sources, allowing tangents of surfaces to be visually evaluated. However, since a linear light source does not occupy a finite area, its reflected image can not be calculated for a shaded image. What the designer needs is a shaded image illuminated by a number of cylindrical light sources. To provide the designer with the feeling of actually being present before a real model, very faithful shading is required.

In most offices, factories, classrooms and stores (and even in most Japanese homes), cylindrical light sources are far more widely used than incandescent lamps. Therefore, for practical lighting design the conventional point light source illumination model is insufficient, and a lighting model for cylindrical light sources is required.

Shadowing is important to grasp the positions of objects. Light sources, other than point or parallel source produce umbra and penumbra. It is very important to duplicate these shadow phenomena in order to generate realistic images. However, calculation of penumbra is time consuming, and calculation of shadows for curved surfaces is complex. Penumbra arise when a portion of the light source as seen from the point being shaded is obscured by some other object in the scene. In essence, calculation of shadows is a type of hidden surface removal. In case of curved surfaces, calculation of shadow is more complicated than polyhedral data. We will demonstrate a method which is applicable to cylindrical, rectangle, and linear sources of illumination.

The method can be outlined as follows:

(1) A scan line method displays curved surfaces accurately, performing hidden surface removal without polygonal approximation.

(2) Shadows, including penumbrae, cast by the curved surfaces are calculated in order to produce a realistic image.

(3) Illuminance is efficiently calculated for multiple parallel cylindrical sources. The resultant image allows the designer to visually evaluate the smoothness and quality of the surface based on the reflected images.

In the following sections, we will survey the previous work, explain the basic idea of our method, describe illuminance, shadow, and specular reflection calculations, and show examples of the results of our method.

2 PREVIOUS WORK

A number of methods for producing images which can be used to evaluate curved surfaces have been proposed. These methods can be classified as either line drawing or shaded image methods. The former methods include surface contouring, lines of curvature, and reflection line. The latter methods include high quality shaded images and curvature maps. Klass(1980) and Farin(1985) evaluated the quality of curved surfaces using highlight curves. Satterfield and Rogers(1984) developed a method for extracting contour lines on B-splines. Dill(1981) developed a method of mapping color-coded curvature maps onto surfaces. Beck *et al.*(1986) analyzed curved surfaces synthetically using contour curves, lines of curvature, and shaded images. Higashi *et al.*(1990) displayed contour curves, lines of curvature, equi-gradient and equi-brightness curves, silhouette patterns, and highlight curves. Saito and Takahashi(1990) demonstrated a method in which the depth and surface normal at each pixel are stored when the image is generated, and then contour curves and pseudo-highlight patterns are extracted and displayed in line drawings generated by image processing techniques. However, line drawings and color fringe drawings are very difficult to appreciate, and appeal only to designers specialists. Shaded images can be far more understandable.

Several researchers have attacked the problem of displaying curved surfaces without polygonal approximation. Kajiya(1982) developed the first ray tracing method for rendering parametrically defined surfaces. His work was followed by many publications addressing ray tracing, including a new ray tracing method for Bézier surfaces presented recently by one of the authors of this paper(Nishita 1990). This method displays trimmed rational Bézier surfaces with high accuracy. We will use a scan line method for hidden surface removal, due to its efficiency over ray tracing. Many scan line algorithms have also appeared, including one by Lane *et al.*(1980) which subdivides the curved surface into polygons at every scan line. The authors recently presented a modification of Lane's method which subdivides surfaces not into polygons, but into subpatches with curved boundaries, which makes for better precision (Nishita 1991).

Next we will outline previous models of linear and finite area light sources. Verbeck and Greenberg(1984) simulated linear and area sources by multiple point sources. However, the method causes aliasing artifacts and results in uneven intensity in the shadow area due to the simulation of a continuous light source as a set of discontinuous point sources. The authors of the current paper derived analytic solutions for the illumination taking into account shadows due to linear sources(Nishita 1985a), area sources and polyhedral sources (Nishita 1983), as well as sky light approximated by a hemispheric light source of large radius (Nishita 1986). These methods are applicable only to convex polyhedral objects. Poulin and Amanatides(1990) derived an analytical solution by integration assuming that the linear light source consists of a collection of point sources on the line segment. It is assumed that point sources have uniform luminous intensity distribution. However, assumption of a uniform distribution is quite restrictive in comparison to actual linear light sources, rendering this model inadequate for practical lighting designs. Many radiosity methods treat area sources. Although the methods yield realistic images, some of them are restricted to polyhedral objects (Nishita 1985b; Baum 1989). Many radiosity methods for curved surfaces adopt sampling methods in calculating emitted light from light sources (Kajiya 1986; Wallace 1989).

3 BASIC CONCEPT

We assume that free-form surfaces are expressed as rational Bézier surfaces. This does not greatly restrict the generality of our method, since most surface representations used in industrial design, including B-splines, can be converted to rational Bézier form. Hidden surface removal is accomplished using the author's scan line method without polygonal approximation (Nishita 1991). This method calculates intersection points between scan lines and surfaces by Bézier Clipping. Bézier Clipping is an iterative method which utilizes the convex hull property of Bézier curves, and converges more robustly to the polynomial's solution than does Newton's method. Bézier clipping method is also used to detect shadow regions cast by curved surfaces.

We assume that light sources are located in parallel on some plane. In other words, rectangles corresponding to light sources are mapped onto a rectangle and rotated to face the calculation point. Light sources are assumed to be perfectly diffuse (i.e., a Lambertian distribution).

Before detecting shadows at a point, we extract obstacles between the point and the plane on which the light sources are arrayed. The data is hierarchically structured for efficiency in later calculations, allowing groups of lights to be considered together.

Diffuse and specular reflections are both taken into account in intensity calculations. In order to evaluate the smoothness of a curved surface, it is sometimes desirable to move the light source.

The procedure can be outlined as follows:

(1) Surface control points are perspective transformed.

(2) Hidden surfaces are removed by a scan line method (Nishita 1991).

(3) Surfaces casting shadows are extracted.

(4) Contribution of each light source to intensity of the surfaces is calculated.

In this paper, we will focus our discussion on steps 3 and 4.

4 INTENSITY CALCULATION

The process will be easier to understand if we explain step 4 first. There are many types of light source models, including point sources which possess only a location, linear sources which have a length, area sources which occupy a finite area, and polyhedral sources which occupy a finite volume.

Consider an area source. If a source is perfectly diffuse and has uniform luminous intensity distribution, the intensity at a point P can be calculated as follows: The source is first projected onto the surface of a hemisphere centered on P, then onto the bottom of the hemisphere. The intensity due to the light source is proportional to the area projected onto the bottom of the hemisphere. If the source is a n sided polygon, the calculation is simple; the following contour integral can be employed(see Fig. 1).

$$I = I_0/2 \sum_{i=1}^{n} \beta_i \cos \delta_i, \tag{1}$$

Here I_0 is luminous intensity of the light source, β_i is the angle between vectors PQ_i and PQ_{i+1}, and δ_i is the angle between the normal of triangle Q_iPQ_{i+1} and the normal of the plane including point P.

For light sources which occupy a volume, the contour line viewed from the point being shaded is regarded as an area source in calculating the intensity. (See reference (Nishita 1983)). for the treatment of polyhedral sources.) For a cylindrical light source, the disks at the ends of the cylinder are generally quite small compared to the projected area of the cylinder, and in any case, for actual fluorescent lamps they are generally covered by the lamp housing. Thus, a perfectly diffuse cylindrical light source can be regarded as a rectangle, so equation (1) is applicable. Consider the rectangle whose center coincides with that of the cylinder, and whose width d is equal to that of the cylinder. The rectangle must be rotated about its center line so that it faces the point being shaded. After rotation, the contour can be handled as a long slender rectangular light source.

A rectangular light source differs from a cylindrical light source only in the sense that its projected width varies depending on viewing direction, while that of a cylinder is invariant. As shown in Fig. 2, cylindrical light sources are arrayed on a large rectangle, parallel to one of its edges (we refer to this plane as the *C-plane*). The vertices of the C-plane are Q_{00}, Q_{01}, Q_{11}, and Q_{10}. The light sources can then be treated as rectangles mapped onto the C-plane. Consider the intensity

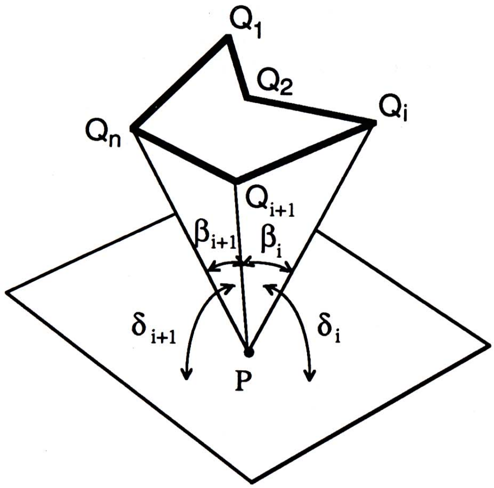

Figure 1: Intensity due to area source by contour integral.

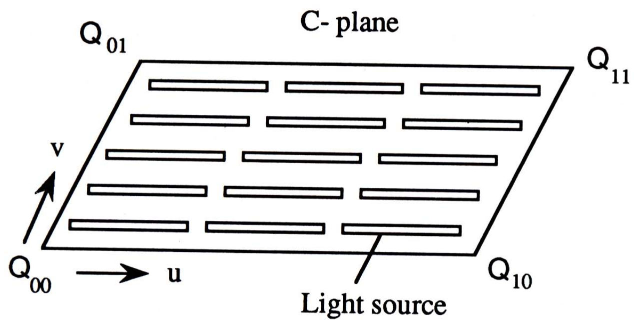

Figure 2: Allocation of light sources.

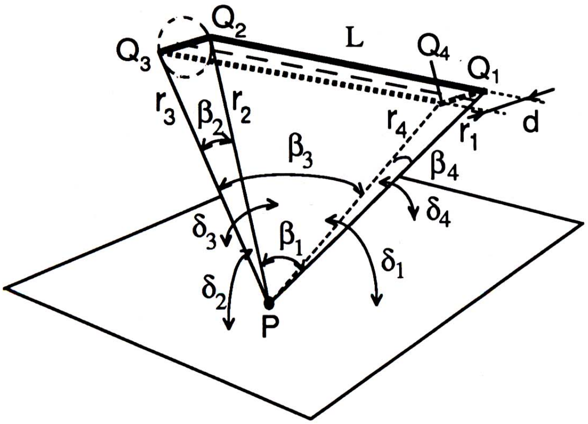

Figure 3: Intensity due to rectangular light source.

at point P illuminated by rotated rectangular light source $Q_1Q_2Q_3Q_4$ on the C-plane (Fig. 3). The lengths of Q_1Q_2 and Q_3Q_4 are equal because of a cylindrical source, and are much longer than the widths, Q_1Q_4 and Q_2Q_3. r_1 and r_4, the distances from P to Q_1 and Q_4, are equal, as are r_2 and r_3. The light source width, *d*, is small enough to consider angles Q_1PQ_2 and Q_3PQ_4 to be equal. Call these angles expressed by β_1 and β_3. Then equation (1) can be written as:

$$I = I_0/2\{(\cos\delta_1 - \cos\delta_3)\beta_1 + \beta_2\cos\delta_2 + \beta_4\cos\delta_4\}. \tag{2}$$

When d is very small compared to r_1, r_2, r_3 and r_4, β_2 and β_4 can be approximated by $\beta_2 = d/r_2$, $\beta_4 = d/r_4$. In general, a number of light sources will be colinear, and thus have the same value of $(\cos\delta_1 - \cos\delta_3)$.

When the light source lies partially below the plane including the point P, P receives light only from the exposed portion of the source, which must therefore be divided into two parts based on the plane. When there are obstacles between P and the light source, shadows must be calculated, as discussed in the following section. A light source may be obscured by the other sources viewed from the calculation point when the calculation point is close to the C-plane. In this case we neglected the calculation of shadow effect.

5 SHADOWS

When the light source as viewed from the point to shade is partially obstructed, the visible portion of the light source must be calculated. Because the width of the rectangular light source simulating a cylindrical light source is generally quite small relative to its length, we perform the visibility calculation as if it were a linear light source. After all visible parts of the linear source are calculated, each visible part is regarded as the new rectangular source, and equation (2) is applied. The process of dividing a linear light source which is partially obstructed does not change δ_1 or δ_3. Extracting segments of the linear source visible from point P, then summing equation (2) for these segments yields the intensity due to a linear source. The total illuminance is calculated by applying this procedure to all linear sources. When the C-plane lies below the plane including P,

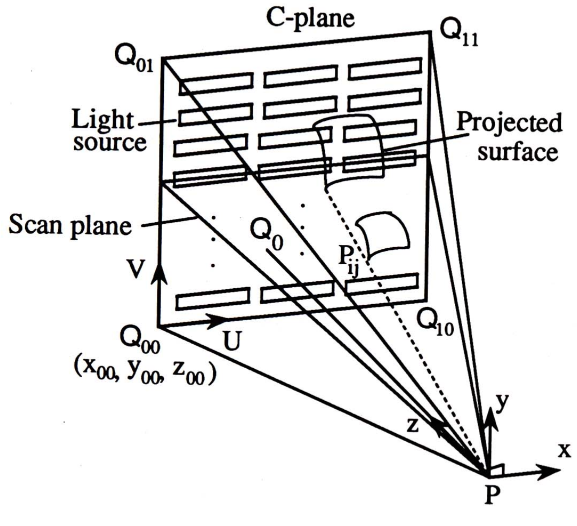

Figure 4: C-plane coordinate system.

the intensity is zero. When a part of the C-plane is below the plane including point P, the lower part of the linear source is clipped away. Extraction of visible parts when dealing with curved surfaces is not easy. Therefore, before detecting shadows due to linear sources, the curved surfaces likely to cast shadows are extracted in advance. We utilize the fact that the C-plane bounds a set of light sources; surfaces likely to cast shadows lie within the pyramid consisting of point P and the C-plane. By treating P as a viewpoint and C-plane as a screen, the linear sources (which are parallel to a side of the C-plane) correspond to scan lines on the screen. Thus, scan line based hidden surface removal algorithms can be used to extract visible portions of the linear light sources.

5.1 Extraction of Curved Surfaces Casting Shadows

First, in order to simplify calculation, we translate the coordinate system to locate P at the origin, and rotate it so that the x and y axes are parallel to the sides $Q_{00}Q_{10}$ and $Q_{00}Q_{01}$ of the C-plane (the light sources are assumed to be parallel to $Q_{00}Q_{10}$)(see Fig. 4). We also define unit vectors **U** and **V** parallel to these edges.

After rotation the y component of **U** is zero, P is a viewpoint, the z axis is the normal of the projection plane, and the C-plane is the screen perpendicular to the z axis. In other words, the pyramid whose bottom is the C-plane and whose apex is P becomes the field of view. We refer to this coordinate system as the *C-plane coordinate system.* Note that Q_0, the intersection of the z axis with the screen, might even not lie between $Q_{00}Q_{01}$ $Q_{11}Q_{10}$)(Fig. 4).

Bézier surfaces are bounded by the convex hull of their control points. We use this property to detect surfaces within the pyramid which may obstruct light based on the relation of each surface's control points to the four sides of the pyramid.

Expressing the control points of a Bézier surface of degree n after transformation into the C-plane coordinate system as (X_{ij}, Y_{ij}, Z_{ij}), and the weights as W_{ij}, the surface is expressed by

$$X(u,v) = \frac{\sum_{i=0}^{n}\sum_{j=0}^{n} W_{ij}X_{ij}B_i^n(u)B_j^n(v)}{\sum_{i=0}^{n}\sum_{j=0}^{n} W_{ij}B_i^n(u)B_j^n(v)}$$

$$Y(u,v) = \frac{\sum_{i=0}^{n}\sum_{j=0}^{n} W_{ij}Y_{ij}B_i^n(u)B_j^n(v)}{\sum_{i=0}^{n}\sum_{j=0}^{n} W_{ij}B_i^n(u)B_j^n(v)} \tag{3}$$

$$Z(u,v) = \frac{\sum_{i=0}^{n}\sum_{j=0}^{n} W_{ij}Z_{ij}B_i^n(u)B_j^n(v)}{\sum_{i=0}^{n}\sum_{j=0}^{n} W_{ij}B_i^n(u)B_j^n(v)}$$

where B is the Bernstein polynomial, given by

$$B_i^n(u) = \binom{n}{i}u^i(1-u)^{n-i}.$$

Consider the plane determined by P and vertices Q_{00} and Q_{01} of the C-plane, and let the distance from point P to the screen be z_0. If all control points $P_{ij}(X_{ij}, Y_{ij}, Z_{ij})$ of a surface satisfy the following equation, the surface lies outside the pyramid.

$$X_{ij} - (x_{00}/z_0)Z_{ij} < 0 \tag{4}$$

Each surface can be checked against any of the pyramid's sides in the same manner.

Because the direction of the axes of the C-plane coordinate system are independent of P, rotation of control points need only be performed once, and each point can be processed with only a translation of the control points to bring the point to the origin.

The y component of a control point projected onto the screen is $z_0 Y_{ij}/Z_{ij}$. Thus, surfaces which interrupt light are easily located using the calculated maximum and minimum y values of control points.

5.2 Extraction of Visible Part of Light Source

As discussed above, light sources are considered to lie on scan lines, so a visibility calculation performed for scan lines yields the visible portions of the light sources. Let the y coordinate of a scan line be y_s. Regions of the "screen" which may be obstructed have already been calculated based on surface control points, so surfaces which may overlap a scan line can be very quickly located. For each such surface, the following test is performed.

The distance between an arbitrary point (X, Y, Z) and the scan plane is proportional to the function

$$d(X,Y,Z) = Y - y_s/z_0 Z. \tag{5}$$

For points located on the scan plane, $d = 0$. Substituting equation (4) into (5) yields

$$d = \sum_{i=0}^{n}\sum_{j=0}^{n} W_{ij}d_{ij}B_i^n(u)B_j^n(v) = 0. \tag{6}$$

where d_{ij} ($= Y_{ij} - y_s/z_0 Z_{ij}$) is proportional to the distance between control point P_{ij} and the scan plane. The intervals of u and v satisfying equation (6) are extracted by Bézier Clipping (Nishita 1990, 1991).

Discarding portions outside these intervals yields a subpatch. If the u and v intervals are not sufficiently shortened, the surface is divided and Bézier Clipping is again applied. This process is iterated until the subpatch is sufficiently flat (Fig. 5). Next, intersections of these subpatches with the scan line are calculated. For example, on the $v = 0$ edge of a subpatch, substituting $v = 0$ in equation (6) and the u which satisfies $d = 0$ is found by Bézier clipping. If d_{ij} for all of a subpatch's control points are of the same sign, the subpatch does not intersect the scan line. Further, because subpatches lying behind point P are irrelevant, the subpatches whose control points have $z < 0$ are discarded.

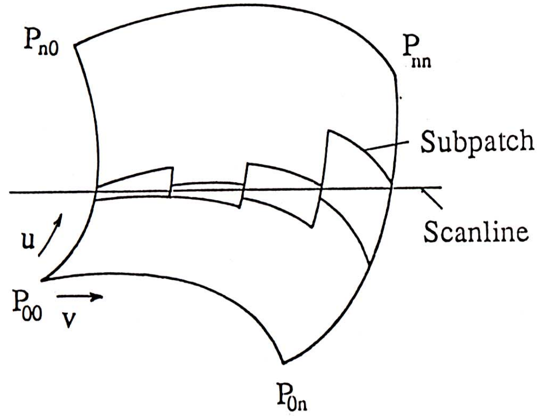

Figure 5: Subpatches on a scanline.

After the intersection point of a subpatch and a scan line is found, its x and z coordinates are used to locate the intersection projected on the screen (i.e., $z_0 x/z$). From these intersections, the visibility intervals of the scan line (which represents a linear light source) are obtained. Quantitative invisibility is used to determine the visible intervals (Appel 1967).

6 CALCULATION OF SPECULAR REFLECTION

The specular reflection is calculated only over visible intervals of light sources obtained by the method described in section 5. This calculation includes calculation of reflected sources on surfaces with high reflectance. As shown in Fig. 6, the specular component is calculated by integrating the incident light weighted with a distribution function centered on the specular reflection vector,**R**. The intensity of the specular component at point P due to the source is obtained by integrating light from differential area dS including point Q on the source.

$$\mathrm{I}_s = k_0 \int_S \mathrm{I}_0 \frac{\cos\alpha}{r^2} \rho dS, \tag{7}$$

where k_0 is the specular reflection component of reflectance, I_0 is the luminous intensity per unit area of the light source, r is the distance between points P and Q, α is the angle between QP and the normal of the source, and ρ is a distribution function. Here we use the distribution function of the Phong model (Phong 1975). In this model, $\rho = (\cos\theta)^n$; θ is the angle between the reflection vector **R** and PQ(we refer the vector PQ as $\mathbf{Lq}$; $\cos\theta = (\mathbf{R}\cdot\mathbf{Lq})$) , and n is the reflection characteristic(associated with the surface roughness); a larger n produces a narrower highlight. Note that $\cos\alpha/r^2 dS$ is equivalent to the solid angle of differential area dS.

Let's consider a single rectangular(band) source. Let the center line of the source be x'-axis, the length of the source L, width direction y', and the width of the source d. Since $dS = dx'dy'$, the intensity of the specular component at P is then rewritten as

$$\mathrm{I}_s = k_0 \mathrm{I}_0 \int_0^L \int_{-d/2}^{d/2} \frac{\cos\alpha}{r^2} (\mathbf{R}\cdot\mathbf{Lq})^n dy' dx'. \tag{8}$$

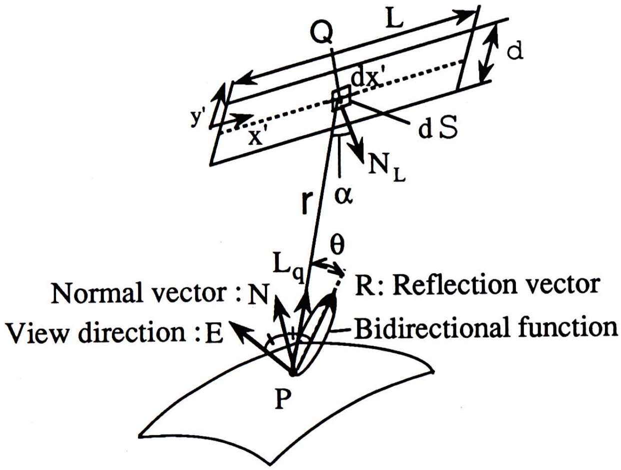

Figure 6: Specular reflection due to rectangular source.

The above equation is solved by numerical integration. Since the width of the source is generally small, $\cos\alpha/r^2$ is regarded as constant for y-direction; the equation is discretized by the following equation.

$$\mathrm{I}_s = k_0 \mathrm{I}_0 \sum_i \frac{\cos\alpha_i}{r_i^2} \sum_j (\mathbf{R}\cdot\mathbf{Lq_{ij}})^n \Delta y_j \Delta x_i, \tag{9}$$

where Δy and Δx are integration(sampling) intervals. Let the intersection point between the specular reflection ray and the C-plane be $P_0(x_0, y_0, z_0)$ (see Fig. 7). The point from which intensity at P is strongest is the nearest point(P_1 in Fig. 7) of the source to P_0, which is the intersection between the source and the line $x = x_0$. The value of $(\cos\theta)^n$ decrease sharply depending on any decrease(or increase) of x. Then integration is started at $x = x_0$ after subdividing the source at $x = x_0$ into two segments. If the value of $\cos\theta$ becomes less than a given tolerance ϵ_1, the calculation is stopped.

For y'-component, $\cos\theta$ is calculated at the center line of the source. If its value is larger than a given value ϵ_2 the sampling points for the calculation of $\cos\theta$ are added. If its value is smaller, however, than a given tolerance ϵ_1, the calculation is stopped. By this method, integration is performed adaptively and only in the limited regions. For a highly specular surface, the integration region is very small, then $\cos\alpha/r^2$ is regarded as a constant over the whole region.

The luminous distribution of a cylindrical (or linear) surface differs little from that of a rectangular one. That is, even though the normal of the rectangular source is fixed, the normal of the cylindrical source rotates so as to exist within the plane including the calculation point P and the center line of the source, because the cylindrical source is assumed as a rotated rectangular one as mentioned before. In other words, the intensity of the cylindrical source can be calculated by substituting $\sin\alpha'$ for $\cos\alpha$ in equation (9); α' is the angle between the center line of the source and $\mathbf{Lq}$.

The efficiency of the calculation is increased by restricting the region to be integrated as follows. The intersection of the C-plane with the circular cone containing the reflection distribution is determined, and the integration is performed only for light sources within the bounding box of the region (see Fig. 7).

Let the intersection point between the specular reflection ray and the C-plane be (x_0, y_0, z_0), and

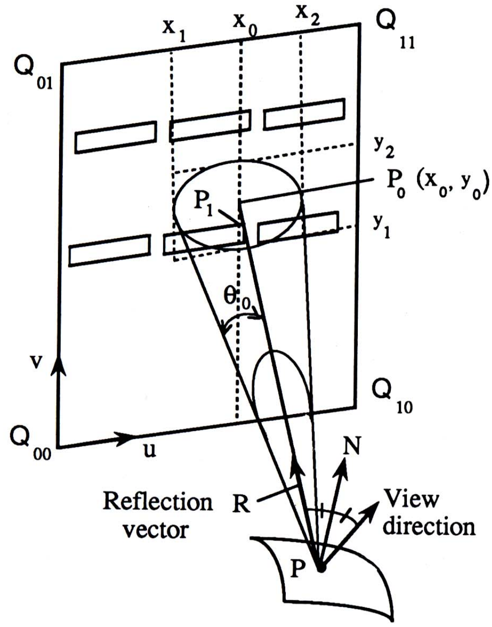

Figure 7: Calculation range for specular reflection.

let the apex angle of the circular cone be θ_0; θ_0 is determined by the relation, $\cos\theta_0 = \epsilon_1^{\frac{1}{n}}$. The bounding box on the C-plane ($[x_1, x_2]$, $[y_1, y_2]$) is expressed by the following equations.

$$\begin{aligned} x_1 &= (x_0 - z_0\tan\theta_0)/(1 + x_0/z_0\tan\theta_0) \\ x_2 &= (x_0 + z_0\tan\theta_0)/(1 - x_0/z_0\tan\theta_0) \\ y_1 &= (y_0 - z_0\tan\theta_0)/(1 + y_0/z_0\tan\theta_0) \\ y_2 &= (y_0 + z_0\tan\theta_0)/(1 - y_0/z_0\tan\theta_0) \end{aligned} \tag{10}$$

The integration is performed only over visible intervals of light sources within this bounding box.

6.1 Positioning Light Sources

When using the reflected image of a light source to evaluate the smoothness of a curved surface, the position of the light relative to the surface must be adjusted. This can be achieved either by translating the light source or by rotating the surface. We will discuss translation of the light source here.

For a given viewpoint and view angle, the angular range covered by the specular reflection cones of all visible surfaces in the scene is in general quite large, making it difficult to set the position of the lights. If no restriction is put on the angle and position of C-plane, there are so many degrees of freedom that the C-plane can not be set up. In fact, the actual physical setup with which designers are accustomed to evaluating surfaces of physical models is quite large (generally occupying the entire ceiling and/or one wall of the room), and therefore cannot easily be rotated to an arbitrary position. Therefore, in this simulation we specify a slope. This slope determines a reference plane, on which the C-plane can be translated. Generally, the reference plane will be set either horizontally or vertically. The orientation of light sources on the plane can be freely rotated. The reference plane is then divided into small regions and the number of reflected rays striking each region is counted. C-planes are set on regions where the number of hits exceeds some threshold.

In order to reduce shadow calculation time, hidden surface removal and calculation of reflected specular rays are performed in advance, without considering shadows. The reference plane is divided into a grid. For a given viewpoint and view angle, the specular rays from all visible surfaces are intersected with the reference plane, and the number of rays striking each grid element is calculated.

7 EXAMPLES

A simple example of a curved surface is shown in Fig. 8. The curved surface is illuminated by 48 (4 rows of 12 columns) cylindrical light sources. The reflected images of lights are obtained by calculating specular component as a highly specular surface. The parallel intensity gradations visible in the penumbra area are due to the parallel located light sources; the stripes appear in shadows because shadowing is done by assuming linear light sources (This artifact may be reduced if a cylindrical light source is approximated by multiple linear light sources).

Figure 9 shows a close-up of the car's front hood in Fig. 10. In (a) contour lines and patch boundaries are drawn. In this figure we can observe smooth continuity of patches, but we can not find irregularity of surfaces. In (b), the hood is illuminated only by a point source, and appears to be smooth. However, the reflected images of light sources visible in (c) reveals problems in the smoothness of the surface.

Figure 10 shows a commercial application, an automobile composed of 204 Bézier patches. This figure shows the car illuminated by 12 long cylindrical sources. The appearance of the penumbra on the floor is very realistic.

As an example of a lighting simulation, Fig. 11 shows a conference room composed of 1127 Bézier patches illuminated by 48 cylindrical sources(6 rows of 4 columns, 2 sources in a case). Illuminance calculation on the ceiling is ignored, and is set constant value. On the desks the highlights due to specular reflection of cylindrical sources are observed. This method gives us realistic images, but calculation of interreflection of light(i.e., radiosity) may be desired for precise lighting simulation.

These images were calculated on a NEC EWS4800/260 workstation. For Fig. 10, hidden surface removal was accomplished in 35.0 seconds, while shading with the cylindrical light sources required 181.9 minutes. For Fig. 11, hidden surface removal was accomplished in 22.0 seconds, while shading with the cylindrical light sources required 53.5 minutes.

In these examples the multi-scanning method (Nakamae 1986) developed by the authors was used for anti-aliasing.

8 CONCLUSION

The parallel cylindrical light source shading model is useful for evaluating the smoothness of curved surfaces and for lighting design. The advantages of the proposed method are as follows:

(1) The curved surfaces are displayed faithfully, without polygonal approximation. As a result, the reflected images of cylindrical light sources provide effective information for visually, intuitively evaluating the smoothness of the surfaces.

(2) Many cylindrical light sources (linear light sources and rectangle light sources) are located in parallel on a plane. Treating this plane as an area source is very effective for increasing the

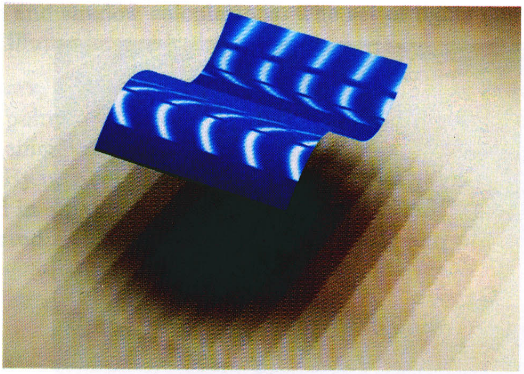

Figure 8: An example of a single patch.

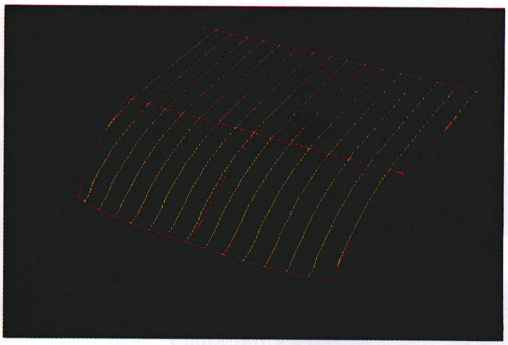

(a) Contour lines.

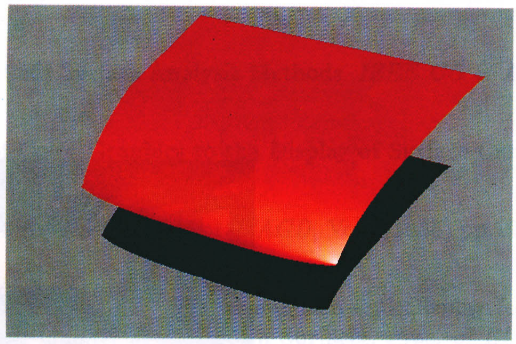

(b) Point light sources.

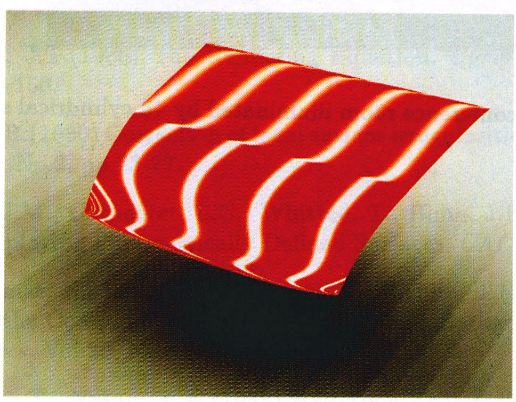

(c) Cylindrical light sources.

Figure 9: Comparison of display methods.

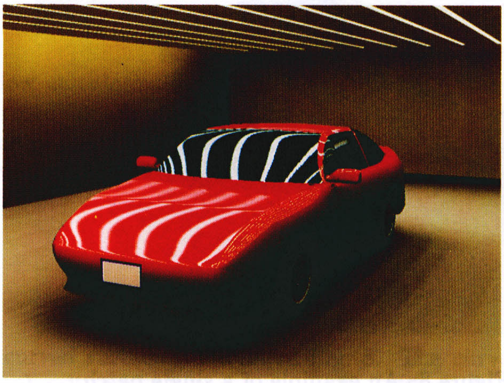

Figure 10: An automobile illuminated by parallel cylindrical sources.

Figure 11: A conference room illuminated by 48 cylindrical sources.

efficiency of illuminance and shadow calculations. The set of lights can be treated as texture thus reducing the amount of illuminance calculation.

(3) Calculation of shadows, in particular of penumbrae, requires extracting the parts of the light sources visible from the point being shaded. By regarding the point as a viewpoint and each linear source as a scan line, an efficient scan line based hidden surface removal algorithm can be applied to calculation of shadows. By utilizing the convex hull property, those patches which are likely to cast shadows are determined in advance. Moreover, tests for intersection between linear light sources (i.e., scan lines) and curved surfaces are performed robustly and accurately by Bézier Clipping.

REFERENCES

[Appel 1967] Appel, A., (1967) The Notion of Quantitative invisibility and the Machine rendering of Solids. *Proc. of the ACM National Conference*, pp.387-393.

[Baum 1989] Baum, D.R., Rushmeier H. E., Winget, J. M.(1989) Improving Radiosity Solutions Through the Use of Analytically Determined Form-Factors. *Computer Graphics*, Vol.23, No.3, pp.325-334.

[Beck 1986] Beck, J., Farouski, T., Hinds, J.(1986) Surface Analysis Methods. *IEEE CG & A*, Vol.6, No.12, pp.18-36.

[Dill 1981] Dill, J.C.(1981) An Application of Color Graphics to the Display of Surface Curvature. *Computer Graphics*, Vol.15, No.3, pp.153-161.

[Farin 1985] Farin, G.(1985) A modified Clough-Tocher interpolant. *CAGD*, Vol.2(1985) pp.19-27.

[Higashi 1990] Higashi, M., Kushimoto, T., Hosaka, M.(1990) On Formulation and Display for Visualizing Features and Evaluating Quality of Free-Form Surfaces. *Proc. of EUROGRAPHICS'90* pp.299-309.

[Kajiya 1982] Kajiya, J.T.(1982) Ray Tracing Parametric Patches. *Computer Graphics*, Vol.16, No.3, pp.245-254.

[Kajiya 1986] Kajiya, J.T.(1986) The Rendering Equation. *Computer Graphics*, Vol.20, No.4, pp.143-150.

[Klass 1980] Klass, R.(1980) Correction of local surface irregularities using reflection lines. *CAD*, Vol.12, No.2, pp.73-77.

[Lane 1980] Lane, J.M., Carpenter, L.C., Whitted, T., Blinn, J.F. (1980) Scan Line Methods for Displaying Parametrically Defined Surfaces. *CACM*, Vol.23, No.1, pp.23-34.

[Nakamae 1986] Nakamae, E., Harada, K., Ishizaki, T., Nishita, T.(1986) Montage: The overlaying of the Computer Generated Image onto a Background Photograph. *Computer Graphics*, Vol.20, No.3, pp.207-214.

[Nishita 1983] Nishita, T., Nakamae, E.(1983) Half-Tone Representation of 3-D Objects Illuminated by Area Sources or Polyhedron Sources. *IEEE COMPSAC*, pp.237-242.

[Nishita 1985a] Nishita, T., Okamura, I., Nakamae, E.(1985) Shading Model for Point and Linear Sources. *ACM Tog*, Vol.4, No.2, pp.124-146.

[Nishita 1985b] Nishita, T., Nakamae, E.(1985) Continuous Representation of Three Dimensional Objects Taking into Account of Shadows and Interreflection. *Computer Graphics*, Vol.19, No.3, pp.23-30.

[Nishita 1986] Nishita, T., Nakamae, E.(1986) Continuous Representation of Three Dimensional Objects Illuminated by Sky Light. *Computer Graphics*, Vol.20, No.3, pp.125-132.

[Nishita 1990] Nishita, T., Sederberg, T., Kakimoto, M.(1990) Ray Tracing Rational Trimmed Surface Patches. *Computer Graphics*, Vol.24, No.4, pp.337-345.

[Nishita 1991] Nishita, T., Kaneda, K., Nakamae, E.(1991) Scanline algorithm for displaying trimmed surfaces by using Bézier clipping. *The Visual Computer*, Vol.7, No.5-6, pp.269-279.

[Phong 1975] Phong, B.(1975) Illumination for Computer Generated Pictures. *CACM*, Vol.18, No.6, pp.311-317.

[Poulin 1990] Poulin, P., Amanatides, J.(1990) Shading and Shadowing with Linear Light Sources. *EUROGRAPHICS '90*, pp.377-386.

[Saito 1990] Saito, T., Takahashi, T.(1990) Comprehensible Rendering of 3-D Shapes. *Computer Graphics*, Vol.24, No.4, pp.197-206.

[Satterfield 1984] Satterfield S. G., Rogers, D.F.(1984) A Procedure for Generating Contour Lines from B-spline Surfaces. *IEEE CG & A*, Vol.4, No.1, pp.61-74.

[Verbeck 1984] Verbeck, C.P., Greenberg, D.P.(1984) A Comprehensive Light Source Description for Computer Graphics. *IEEE CG & A*, Vol. 4, No. 7, pp. 66-75.

[Wallace 1989] Wallace, J. R., Elmquist, K. A., Haines, E. A.(1989) A Ray Tracing for Progressive Radiosity. *Computer Graphics*, Vol.23, No.3, pp.315-324.

Tomoyuki Nishita is a professor in the department of Electronic and Electrical Engineering at Fukuyama University, Japan. He was on the research staff at Mazda from 1973 to 1979 and worked on design and development of computer-controlled vehicle system. He joined Fukuyama University in 1979. He was an associate researcher in the Engineering Computer Graphics Laboratory at Brigham Young University from 1988 to the end of March, 1989. His research interests involve computer graphics including lighting model, hidden-surface removal, and antialiasing.
Nishita received his BE, ME and Ph. D in Engineering in 1971, 1973, and 1985, respectively, from Hiroshima University. He is a member of ACM, IPS of Japan and IEE of Japan.
Address: Faculty of Engineering, Fukuyama University, Sanzo, Higashimura-cho, Fukuyama, 729-02 Japan.
E-mail: nis@eml.hiroshima-u.ac.jp

Shinichi Takita is a professor in the Department of Education at Kagawa University,Japan. His research interests include computer graphics and CAI.
Takita received his BE and ME degrees in electrical engineering form Hiroshima University in 1964 and 1966, respectively. He is a member of the IEE of Japan and the Japan Society of Industrial and Technical Education.
Address: Faculty of Education, Kagawa University, 1-1, Saiwai-cho, Takamatsu, 760 Japan.

Eihachiro Nakamae is a professor at Hiroshima University where he was appointed as research associate in 1956 and a professor in 1968. He was an associate researcher at Clarkson College of Technology, Potsdam, N. Y., from 1973 to 1974. His research interests include computer graphics and electric machinery.
Nakamae received the BE, ME, and DE degrees in 1954, 1956, and 1967 from Waseda University. He is a member of IEEE, IEE of Japan, IPS of Japan and IEICE of Japan.
Address: Faculty of Engineering, Hiroshima University, Kagamiyama, Higashi-hiroshima, 724 Japan.
E-mail: naka@eml.hiroshima-u.ac.jp